NASA Technical Memorandum 86325

NASA-TM-86325 19850007753

NUMERICAL STUDIES OF INTERACTING VORTICES

Grace C. Liu and Chung-Hao Hsu

JANUARY 1985

National Aeronautics and
Space Administration

Langley Research Center
Hampton, Virginia 23665

SUMMARY

To get a basic understanding of the physics of flowfields modeled by vortex filaments with finite vortical cores, systematic numerical studies of the interactions of two-dimensional vortices and pairs of coaxial axisymmetric circular vortex rings were made. Finite-difference solutions of the unsteady incompressible Navier-Stokes equations were carried out using vorticity and stream function as primary variables. Special emphasis was placed on the formulation of appropriate boundary conditions necessary for the calculations in a finite computational domain. Numerical results illustrate the interaction of vortex filaments, demonstrate when and how they merge with each other, and establish the region of validity for an asymptotic analysis.

INTRODUCTION

The vortex core structure, vortex merging, and the intersection of multiple vortex filaments have been of interest for many years. The flows are characterized by time-dependent and three-dimensional interactions.

Mathematical models of vortex filaments have been frequently employed for the explanation of phenomena such as free jet flows [1] and aircraft wakes [2]. Asymptotic analysis is well known to be valid if $\delta/\ell \ll 1$, where δ is the effective viscous core size and ℓ is the characteristic flowfield length. When merging is about to occur, i.e., as the ratio δ/ℓ in the flow becomes no longer small, the asymptotic theory may not be applicable. To continue the study of flowfields dominated by interacting vortex filaments, numerical solutions of the Navier-Stokes equations must be carried out.

One of the main difficulties in numerical simulation of a flowfield in an unbounded domain is how to formulate appropriate boundary conditions necessary for solving the Navier-Stokes equations in a finite computational domain. In order to avoid a large computational domain, a method of specifying boundary conditions on a bounded domain with error control has been presented in [3]. Based on integral properties of the solution, this method allows the size of the computational domain to be reduced until the error introduced at the boundary approaches the same order of magnitude as that of the finite-difference approximation. Variations in the application of this efficient boundary condition method have been reported in [2,4-8].

To study the motion and merging of vortex filaments, the unsteady incompressible Navier-Stokes equations with aforementioned efficient boundary conditions are solved. The time variation of contour lines of constant vorticity illustrates the motion and merging of vortices. A much better picture of merging can be seen with graphs of trajectories of the locations of maximum vorticity and with graphs of the decay of maximum vorticity with respect to time. The practical limit for δ/ℓ in the asymptotic theory is also shown. Cases included are (1) two, three, and four two-dimensional vortices; and (2) two coaxial axisymmetric circular vortex rings.

Subsequent sections of this paper contain a description of the governing equations, a brief discussion of the appropriate boundary conditions, an outline of the computational scheme, and numerical results demonstrating the characteristics of the vortical interactions.

SYMBOLS

$\vec{A}$	vector velocity potential
a	effective radius (centered at the origin) of the vorticity distribution in two-dimensional cases or cross-sectional radius of a vortex ring
e_A	error of approximate boundary data for $\vec{A}$
e_f	error of the finite-difference approximation
e_ω	error due to $\vec{\omega} = 0$ on the boundary
D_o	initial separation distance between two vortex rings
L	size of the computational domain
ℓ	characteristic flowfield length
M	number of two-dimensional interacting vortices
R,Z	cylindrical coordinates
R_e	Reynolds number, Γ/ν
R_o	initial centerline radius of a vortex ring
r	$\lvert\vec{x}\rvert$
t	time scale
t^*	time-shift constant for an optimum single Lamb vortex
t_o	initial time of numerical computation
$\vec{V}$	velocity vector
X,Y	inertial Cartesian coordinates
x,y	rotating Cartesian coordinates fixed on one of the lines through the vorticity maxima
$\vec{x}$	general position vector
$\tilde{\vec{x}}$	location of vortex maximum for asymptotic solutions
Γ	circulation
δ	effective viscous core size

δ_o initial effective viscous core size

ζ scalar vorticity for Navier-Stoke solutions

$\tilde{\zeta}$ scalar vorticity for the sum of asymptotic solutions

ζ^* scalar vorticity for an optimum single Lamb vortex

ν kinematic viscosity

ρ initial distance between the origin and an individual two-dimensional Lamb vortex

$\tilde{\Omega}$ instantaneous angular speed of the x-axis

$\vec{\omega}$ vorticity vector

$\vec{\omega}_o$ initial vorticity distribution

GOVERNING EQUATIONS

Incompressible laminar flowfields induced by initial vorticity distributions are governed by

$$\nabla \cdot \vec{V} = 0 \tag{1}$$

$$\vec{\omega}_t + (\vec{V} \cdot \nabla)\vec{\omega} - (\vec{\omega} \cdot \nabla)\vec{V} = \nu \Delta \vec{\omega} \tag{2}$$

$$\vec{\omega} = \nabla \times \vec{V} \tag{3}$$

subject to the initial condition

$$\vec{\omega}(\vec{x},0) = \vec{\omega}_o(\vec{x}) \tag{4}$$

and the boundary condition.

$$\vec{V}(\vec{x},t) \to 0 \quad \text{as} \quad |\vec{x}| \to \infty \tag{5}$$

For a flowfield dominated by vortices, the initial data $\vec{\omega}_o$ are either of bounded support or decay exponentially in r, where $r = |\vec{x}|$. As a result, the vorticity decays exponentially in r for all $t > 0$, that is

$$\vec{\omega}(\vec{x},t) = O(e^{-br}) \tag{6}$$

for some positive constant b. Equations (1) to (5) define an initial-value problem in an unbounded domain for $\vec{\omega}$ and $\vec{V}$.

The divergence-free condition of the velocity field, equation (1), allows $\vec{V}$ to relate to its vector velocity potential $\vec{A}$ by

$$\vec{V} = \nabla \times \vec{A} \tag{7}$$

After imposing $\nabla \cdot \vec{V} = 0$, $\vec{A}$ then fulfills the vector Poisson equation

$$\Delta \vec{A} = -\vec{\omega} \tag{8}$$

The governing equations are now (2), (7), and (8) with $\vec{\omega}$ and $\vec{A}$ as prime variables. At each instant, the vector velocity potential $\vec{A}$, i.e., the solution of equation (8) with boundary condition (5), can then be related to $\vec{\omega}$ in an unbounded domain by the Poisson integral

$$\vec{A}(\vec{x},t) = \frac{1}{4\pi} \iiint_{-\infty}^{\infty} \frac{\vec{\omega}(\vec{x}',t)}{|\vec{x} - \vec{x}'|} d\vec{x}' \tag{9}$$

Since numerical calculations can only be performed in a bounded domain, appropriate boundary conditions for $\vec{\omega}$ and $\vec{A}$ must be introduced. It is assumed that $\vec{\omega} = 0$ outside of the domain and that

$$\vec{\omega} = 0 \qquad \text{on the boundary.} \tag{10}$$

According to condition (6), the error of this approximation e_ω is on the order of e^{-bL} with L as the size of the finite computational domain. The error of the finite-difference approximation e_f depends on the numerical scheme. By matching e_f with e_ω, L can be chosen so that the approximate boundary conditon for $\vec{\omega}$, equation (10), is acceptable.

This is the approach employed for the two-dimensional problems in [9,10]. It is noted that for the two-dimensional or axisymmetric case the vector velocity potential $\vec{A}$ has only one component, i.e., the scalar stream function, and the vector vorticity $\vec{\omega}$ also has only one component, i.e., the scalar vorticity ζ. The evaluation of a Poisson integral is extremely time consuming even for two-dimensional problems. It will become worse for three-dimensional problems, because the number of operations is $O(N^6)$ for a grid with N points in each direction. Even if the Poisson integral is used to evaluate the boundary data for $\vec{A}$ and the Poisson solver [11] is applied to the interior domain, it is still very inefficient. The reason is that the number of operations for calculating the domain interior is only $O(N^3 \log N)$ while the number for evaluating the boundary data is $O(N^5)$. The efficient boundary condition specification technique used here was developed by Ting [3] so that the number of operations for establishing the boundary data is $O(N^3)$ and the error e_A introduced at the boundary for $\vec{A}$ is $O(L^{-m})$ with $m>4$.

APPROXIMATE BOUNDARY CONDITIONS FOR VECTOR VELOCITY POTENTIAL

To generate more accurate boundary data for $\vec{A}$, the farfield behavior of the Poisson integral (9) is developed. When the vorticity decays exponentially in the farfield, $\vec{A}$ can be represented as a power series in r^{-1} by expanding the denominator of the Poisson integral. The coefficients of the terms in the power series are moments of the vorticity distribution. The first moments and several linear combinations of higher moments are time-invariant. These results [3] are used to determine the boundary data for numerical solutions. Time-invariant moments of vorticity distributions can also be used to monitor the global accuracy of the finite-difference solutions.

The error of approximate boundary data for $\vec{A}$ is $e_A = O(L^{-m})$ and m depends on the number of terms used in the power series. By matching e_f with e_A, which is usually much larger than e_ω, the optimal size of the computational domain is determined.

The appropriate boundary conditions for $\vec{A}$ in the general three-dimensional case are presented in [3]. They can be reduced to the two-dimensional case [2, 3] or the axisymmetric case [3, 4] with proper modifications.

COMPUTATIONAL SCHEME

In two-dimensional cases, the effective radius a (centered at the origin) of the vorticity distribution is required to be sufficiently smaller than the size of the domain L, i.e., $a \ll L$, all the time. In axisymmetric cases, the vorticity distribution is considered to be concentrated almost entirely inside a torus whose cross-sectional radius a is much smaller than its centerline radius R, i.e., $a \ll R$. To study the merging of two vortex rings with very small core radii, the special case where $a \ll L \ll R$ is considered.

Since the vorticity is assumed to decay exponentially in distance, the initial data $\vec{\omega}_o$ are generated by summing several individual Lamb line vortices (asymptotic solutions) and Lamb-type vortex rings for the two-dimensional and axisymmetric problems, respectively. The minimum distance between vortices is sufficiently larger than each individual core size so that asymptotic solutions are valid.

The finite-difference scheme consists of the following steps.

(i) Vorticity integrals are evaluated using Simpson integration over the finite computational domain.

(ii) The boundary data of $\vec{A}$ are calculated by applying the farfield approximations metioned in the previous section.

(iii) A fast Poisson solver is employed to determine $\vec{A}$ in the interior of the computational domain.

(iv) The velocity field $\vec{V}$ is obtained by taking the curl of $\vec{A}$.

(v) The vorticity field $\vec{\omega}$ is advanced in time by integrating the vorticity transport equation (2) in a conservative form using either the Dufort-Frankel scheme or the ADI scheme.

Steps (i) through (v) are repeatedly applied to advance the finite-difference solution in time. In order to attain a time-accurate transient solution to the unsteady flow problem, relatively small time steps must be taken. The time step should also be consistent with the truncation error due to spatial discretization and with the error due to taking only finite terms of farfield approximations for $\vec{A}$. This algorithm is accurate to the second order in space and time.

RESULTS AND DISCUSSION

The unsteady incompressible Navier-Stokes equations with efficient boundary conditions are solved for two-dimensional and axisymmetric interacting vortices. Examples are chosen to demonstrate the merging of vortices and the practical limit of the asymptotic analysis [12-14].

For two-dimensional problems, the merging of M identical vortices located symmetrically on a circle of radius ρ is studied for $M = 2$, 3, and 4. Under

inviscid theory, the vortices will move along the circle at a constant speed. Due to the decay of the vortical core and the enlargement of the effective individual core size, the M points of maximum vorticity will spiral inward faster and faster as the vortical cores overlap each other more and more. Eventually the M points of maximum vorticity coincide at the origin and the constant vorticity lines begin circularizing around the origin.

To carry out the Navier-Stokes solutions, the initial effective core size is set to be 0.5ρ for all cases. Initially the vorticity at the origin is of the order of e^{-4} and can be ignored. The initial core structure for each vortex is that of an isolated Lamb vortex created at $t=0$. The initial core size δ_o is chosen as the unit length scale and $\delta_o^2/4\nu$ as the unit time scale; therefore, numerical computation begins at $t=t_o=1$.

From the Navier-Stokes solutions, the evolution of contour lines of constant vorticity for M vortices is presented in figure 1 for $Re=\Gamma/\nu = 100$ and $M=3$. Figures 1a-1h show the different stages of merging. At each instant, four contour lines at 0.995, $e^{-1/2}$, e^{-1}, and $e^{-3/2}$ times its maximum value, $\zeta_{max}(t)$, are shown. X and Y are the inertial Cartesian coordinates, while x and y are the coordinates rotating with one of the lines through the vorticity maxima. Figure 1a displays the initial contour lines of the three nonoverlapping Lamb vortices. Figure 1b shows that the outermost contour lines of $\zeta = e^{-3/2}\zeta_{max}(t)$ for the three vortices are merging at $t=1.60$. Figures 1c-1e show the successive merging of the inner contour lines one by one at $t=1.90$, 3.11, and 4.02, respectively. For $t>.62$, the three maximum vorticity points merge at the origin and the character of three distinct vortices disappears. Figures 1f-1h then show the gradual circularization of the contours beginning from the inner ones as time increases. In figure 1h, $t=8.24$, all four contour lines are nearly circles. The vorticity should then decay like a single Lamb vortex of strength $M\Gamma$ with an appropriate age defined by an optimum asymptotic solution [10, 14].

When the initial vorticity distribution is defined by the sum of asymptotic solutions for nonoverlapping Lamb vortices, the solution

$$\tilde{\zeta}(x,t)= \frac{\Gamma}{4\pi\nu t} \sum_{j=1}^{M} e^{-[\rho^2+x^2-2\rho x\, \cos(\frac{j-1}{M})2\pi]/4\nu t} \tag{11}$$

is certainly quite accurate at the early stage. However, it is useful to find out how far the asymptotic theory can be extended into the overlapping stage by comparing the solution $\tilde{\zeta}$ with the Navier-Stokes solution ζ. From equation (11), the instantaneous angular speed $\tilde{\Omega}$ of the x-axis (the first line through the maximum $\tilde{\zeta}$) is obtained as

$$\tilde{\Omega}(t)= \frac{\Gamma}{4\pi\rho^2} \sum_{j=2}^{M} \{1-e^{-\rho^2[1-\cos(\frac{j-1}{M}\,2\pi)]/2\nu t}\} \tag{12}$$

From equation (11), the location $\tilde{x}(t)$ for $\tilde{\zeta}_{max}(t)$ is found. Together with equation (12) the trajectory and decay of $\tilde{\zeta}_{max}(t)$ are determined.

Figure 2 illustrates that the difference between the decay of $\tilde{\zeta}_{max}(t)$ obtained from the sum of asymptotic solutions and that of $\zeta_{max}(t)$ from Navier-Stokes solutions becomes noticeable only when merging is taking place. It is surprising

that the $\tilde{\zeta}_{max}$ curve follows very well with the ζ_{max} curve for M=4 even after merging.

Figure 3 indicates the trajectories of the locations of maximum vorticity for Navier-Stokes solutions (solid lines) and for the sum of M asymptotic solutions (dotted lines). The agreements of the trajectories between them become better as M increases; however, the trajectories of inviscid solutions (dash lines) remain as the circle of radius ρ and can never show the merging characteristics at all.

It is found that even when the core size of an individual Lamb vortex is on the order of the distance between vortices, the sum of asymptotic solutions is in good agreement with the Navier-Stokes solution. Also, the agreement remains good for a longer time with larger M. This can only be attributed to the fact that the nonlinear convection terms become smaller and smaller as the number of vortices increases. Without the nonlinear terms, the sum of the asymptotic solutions is the exact solution.

After merging, the Navier-Stokes solutions may be represented by an optimum single Lamb vortex defined by

$$\zeta^*(X,Y,t)= \frac{M\Gamma}{4\pi\nu(t+t^*)} e^{-(X^2+Y^2)/4\nu(t+t^*)} \tag{13}$$

where t^* is a constant time-shift parameter obtained by letting the single vortex have the same polar moment as that of the initial data [10, 14]. This isolated vortex is created at $t=-t^*$, i.e., when it is a point vortex. For the present initial vorticity distribution, it can be shown that

$$t^* = \frac{\rho^2}{4\nu} + t_0 \qquad \text{for all M.} \tag{14}$$

It is equal to 5 when $\nu=0.25$. As shown in figure 2, the agreement between the decay of ζ^*_{max} and that of ζ_{max} becomes better and better as time increases.

For axisymmetric problems, the cylindrical coordinates (R, Z) are used, where R is in the radial direction and Z is on the axis of symmetry. The coordinate frame translates in the Z-direction at an instantaneous inertial speed which is an average of the flowfield velocity weighted by the local magnitude of the vorticity.

Numerical examples for two initially identical coaxial vortex rings of radius $R_o=15$ and of similarity vorticity distribution are carried out to show how and when they will merge into a single vortex ring. The initial core size δ_o is used as the unit length scale. The unit time scale is chosen such that the initial time $t_o=1/4\nu$. The two rings are initially separated by a distance D_o. The Reynolds number based on the initial core size is defined as Γ/ν where Γ denotes the strength of a vortex ring.

Figure 4 illustrates a typical evolution of the vorticity for two right-moving interacting vortex rings with Re=754, ν = 0.25, and $D_o=6$. Note that the displayed vorticity contours represent the vorticity distribution on a meridian plane cutting through the torus with only the contours centered at (R_o, Z) being shown. The center of the torus is under the contours. The first ring, moving ahead initially, is stretching its radius and slowing down. In contrast, the second ring, moving behind

initially, is contracting its radius and speeding up. The plane of the second ring passes over that of the first ring at t=1.83. At this instant, the two rings switch the roles of leading and lagging. It is observed that the two vortex rings cross over each other two more times at t=3.11 and 3.81. Finally, the two rings merge into a single ring for t > 3.81.

Figure 5 shows the decay of maximum vorticity for various initial separation distances D_o=3, 4 and 6 at a fixed Reynolds number of 251. As D_o decreases, the vortical interactions become stronger so that the maximum vorticity decays faster and complete merging occurs sooner. Figure 6 displays the trajectories of the locations of maximum vorticity. The two rings pass over each other once, separate once, and then merge into a single ring in all three cases.

Figure 7 depicts the decay of maximum vorticity for various Reynolds number Re=47, 189, and 754 at a fixed D_o of 6. As Re decreases, the viscous effects become larger so that the maximum vorticity decays faster and complete merging occurs earlier. It should be noted that the time is scaled by the Reynolds number. Figure 8 presents the effect of Reynolds number on the trajectories of the locations of maximum vorticity. The two vortex rings pass over each other three times before merging for Re=754, pass over each other only once before merging for Re=189, and merge into a single ring without passing over each other for Re=47.

The difference of the maximum vorticities between the two rings decreases as Re or D_o decreases. The reason is that the effect due to stretching of the ring diminishes as Re or D_o decreases. Consequently, both curves of the decay of the maximum vorticity for the two rings become closer to that of the corresponding two-dimensional results.

CONCLUSIONS

The unsteady incompressible Navier-Stokes equations have been solved for two-dimensional and axisymmetric interacting vortices. Numerical examples have been chosen to demonstrate the merging characteristics and establish the practical limit of the asymptotic analysis.

For two-dimensional problems, it is found that even when the core size of an individual Lamb vortex is on the order of the distance between vortices, the decay of the maximum vorticity obtained from the sum of asymptotic solutions is in good agreement with that from the Navier-Stokes solutions and the agreement remains longer in time for larger numbers of vortices. When merging is about to take place, numerical solutions of the Navier-Stokes equations are required. After complete merging, the optimum single Lamb vortex solution can represent the Navier-Stokes solution better and better as time increases. The comparison of the trajectory of the locations of maximum vorticity for Navier-Stokes solutions with that for the sum of asymptotic solutions becomes better for larger number of vortices. On the other hand, inviscid theory can neither show the decay of the maximum vorticity nor the correct trajectory of the locations of maximum vorticity.

For axisymmetric problems, numerical results show that as the Reynolds number or the initial separation distance decreases, the effect due to stretching of the vortex ring diminishes so that the maximum vorticity decays faster and complete merging occurs earlier. As the Reynolds number increases, the elapsed times for switching the roles of leading and lagging of the two vortex rings will increase.

ACKNOWLEDGEMENTS

The authors wish to acknowledge Drs. L. Ting and C. H. Liu for several helpful suggestions and discussions. The research work of Dr. C. H. Hsu is supported by the NASA Grant NAG 1-455.

REFERENCES

1. Fung, Y. T. and Liu, C. H., Vortex Simulation of the Pressure Field of a Jet, NASA TM X-73984, 1976.

2. Weston, R. P. and Liu, C. H., Approximate Boundary Condition Procedure for the Two-Dimensional Numerical Solution of Vortex Wakes, AIAA Paper 82-0951, 1982.

3. Ting, L., On the Application of the Integral Invariants and Decay Laws of Vorticity Distributions, Journal of Fluid Mechanics, Vol. 127, pp. 497-506, 1983.

4. Liu, C. H. and Ting, L., Numerical Solutions of Viscous Flow in Unbounded Fluid, Lecture Notes in Physics, Vol. 170, Springer Verlag, pp. 357-363, 1982.

5. Liu, C. H., Thomas, J. L., and Tung, C., Navier-Stokes Calculations for the Vortex Wake of a Rotor in Hover, AIAA Paper 83-1676, 1983.

6. Chamberlain, J. P. and Liu, C. H., Navier-Stokes Calculations for Unsteady Three-Dimensional Vortical Flows in Unbounded Domains, AIAA Paper 84-0418, 1984.

7. Chamberlain, J. P. and Weston, R. P., Three-Dimensional Navier-Stokes Calculations of Multiple Interacting Vortex Rings, AIAA Paper 84-1545, 1984.

8. Liu, C. H., Tavantzis, J., and Ting, L., Numerical Studies of Motion of Vortex Filaments - Implementing the Asymptotic Analysis, AIAA Paper 84-1542, 1984.

9. Wu, J. C. and Thompson, J. F., Numberical Solutions of Time-Dependent Incompressibles Navier-Stokes Equations Using an Entegro-Differential Formulation, Computer and Fluids, Vol. 1, pp. 197-215, 1973.

10. Lo, R.K.C. and Ting, L., Studies of the Merging of Vortices, The Physics of Fluids, Vol. 19, pp.912-913, 1976.

11. Swarztrauber, P. N. and Sweet, R. A., ALGORITHM 541, Efficient FORTRAN Subprograms for the Solution of Separable Elliptic Partial Differential Equations [D3], ACM Transactions on Mathematical Software, Vol. 5, pp. 352-364, 1979.

12. Ting, L. and Tung, C., Motion and Decay of a Vortex in a Non-Uniform Stream, Physics of Fluids, Vol. 8, pp. 1039-1051, 1965.

13. Tung, C. and Ting, L., Motion and Decay of a Vortex Ring, Physics of Fluids, Vol. 10, pp. 901-910, 1967.

14. Ting, L., Studies in the Motion and Decay of Vortices, in Aircraft and Wake Turbulence and Its Detection (Plenum Press, New York) pp. 11-39, 1971.

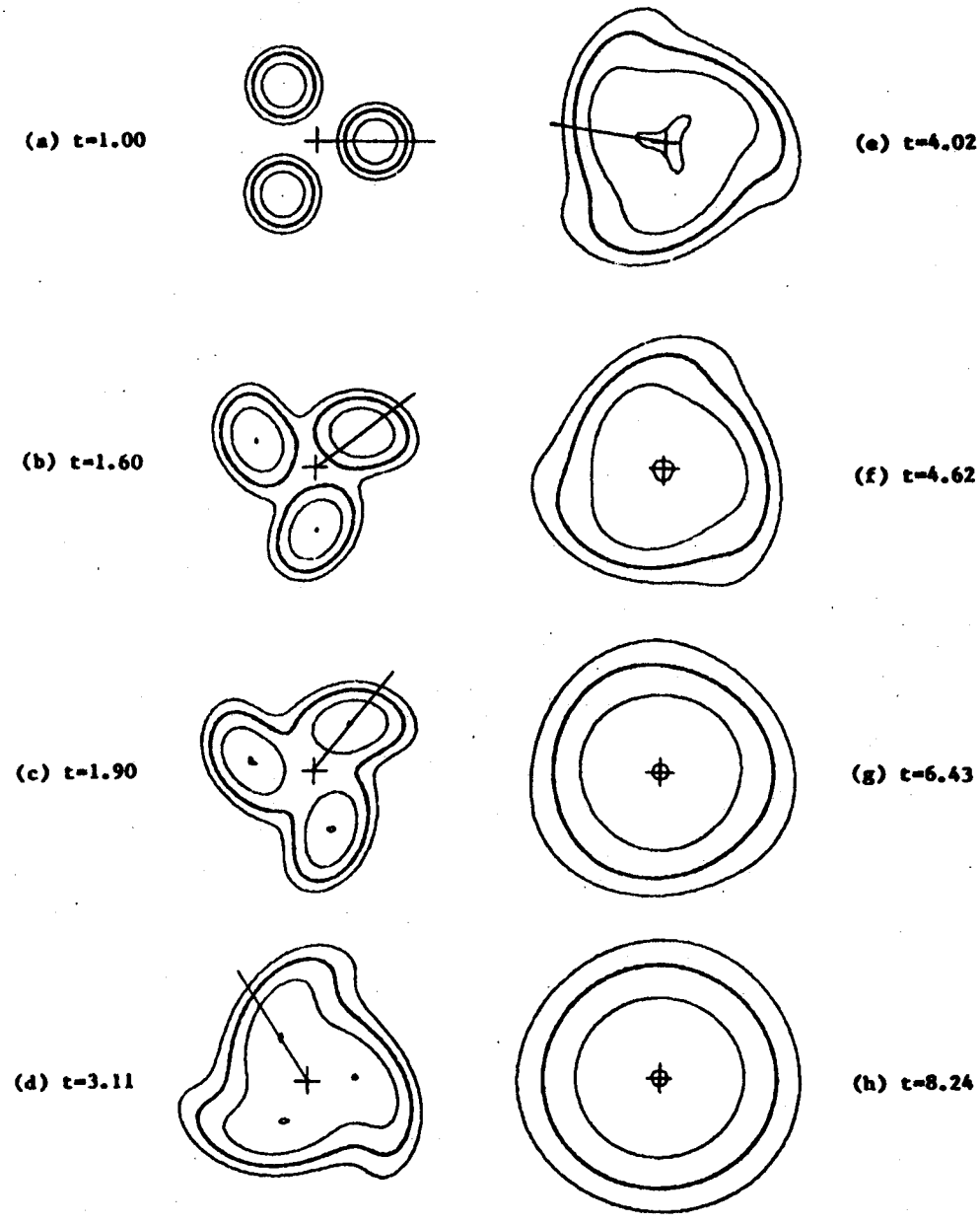

Fig. 1: Vorticity contours for the merging of three two-dimensional vortices of the same sense at Re=100.

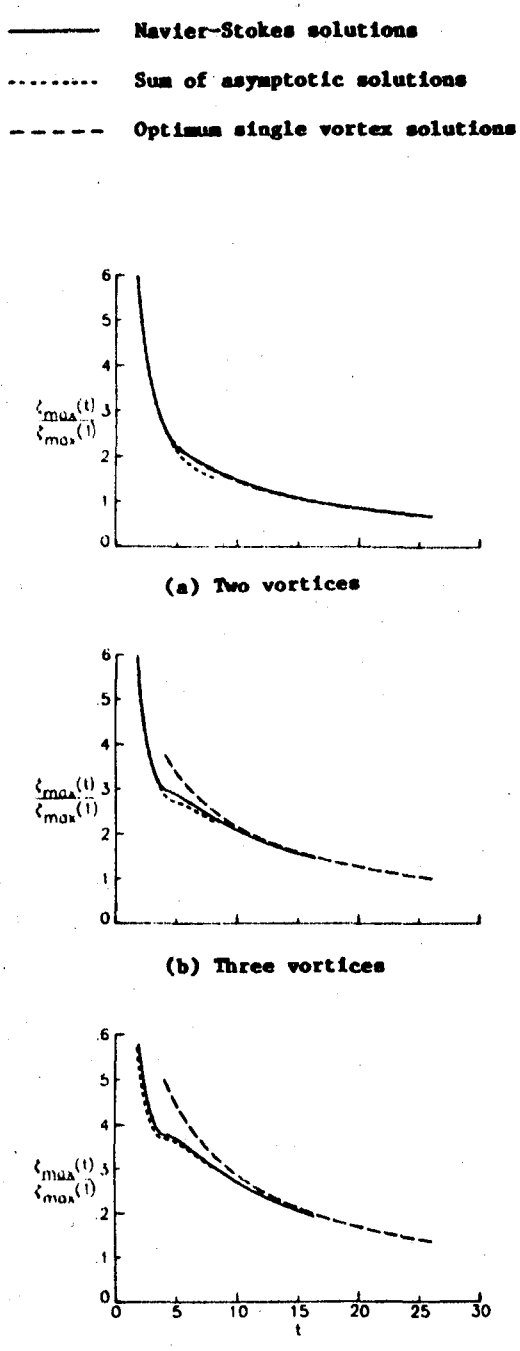

Fig. 2: The decay of maximum vorticity for the merging of multiple two-dimensional vortices at Re=100.

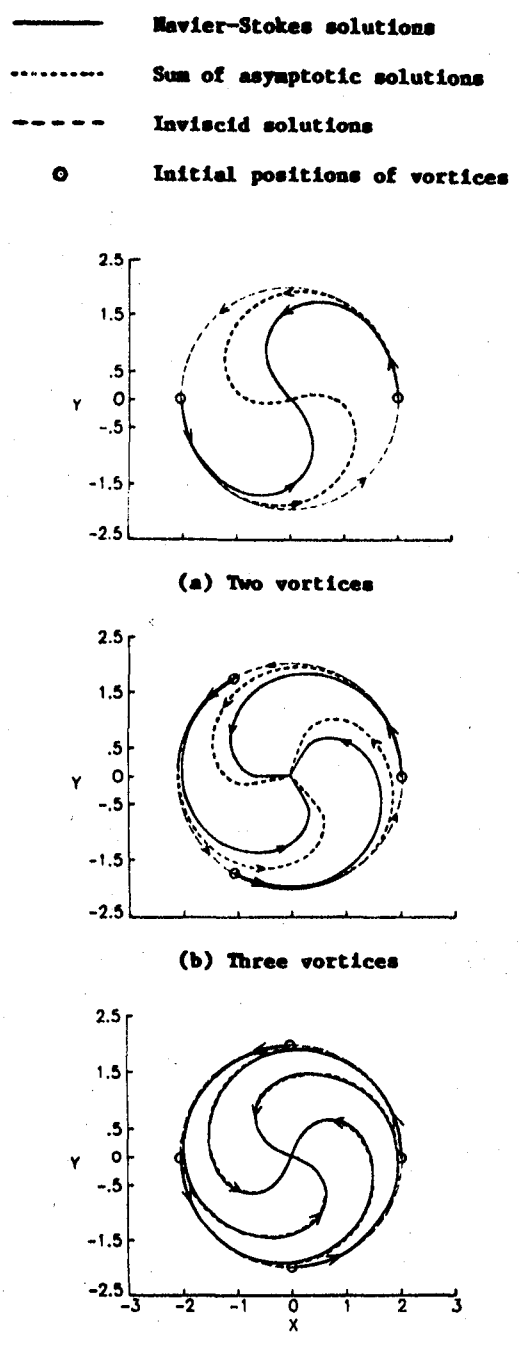

Fig. 3: Trajectories of the location of maximum vorticity for the merging of multiple two-dimensional vortices at Re=100.

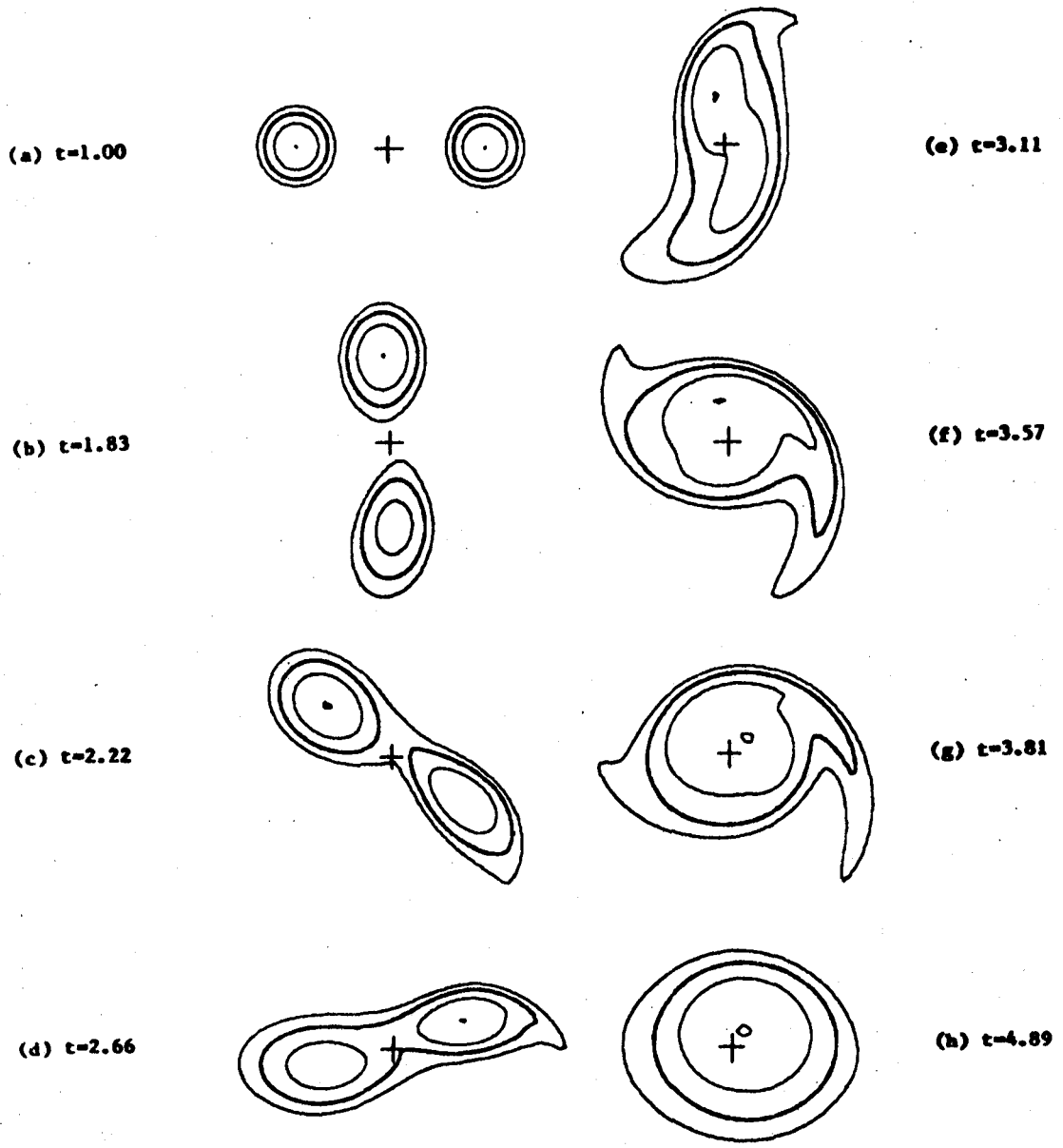

Fig. 4: Vorticity contours of two interacting vortex rings of the same sense with R_0=15 and D_0=6 at Re=754.

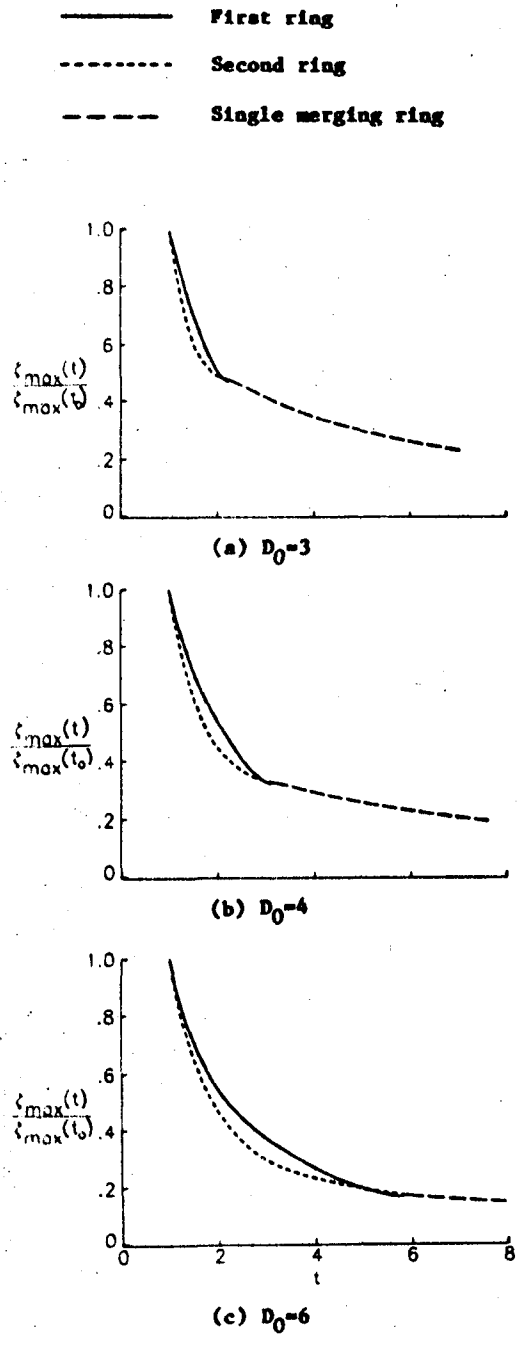

Fig. 5: Effect of initial separation distance on the decay of maximum vorticity for two vortex rings with R_0=15 at Re=251.

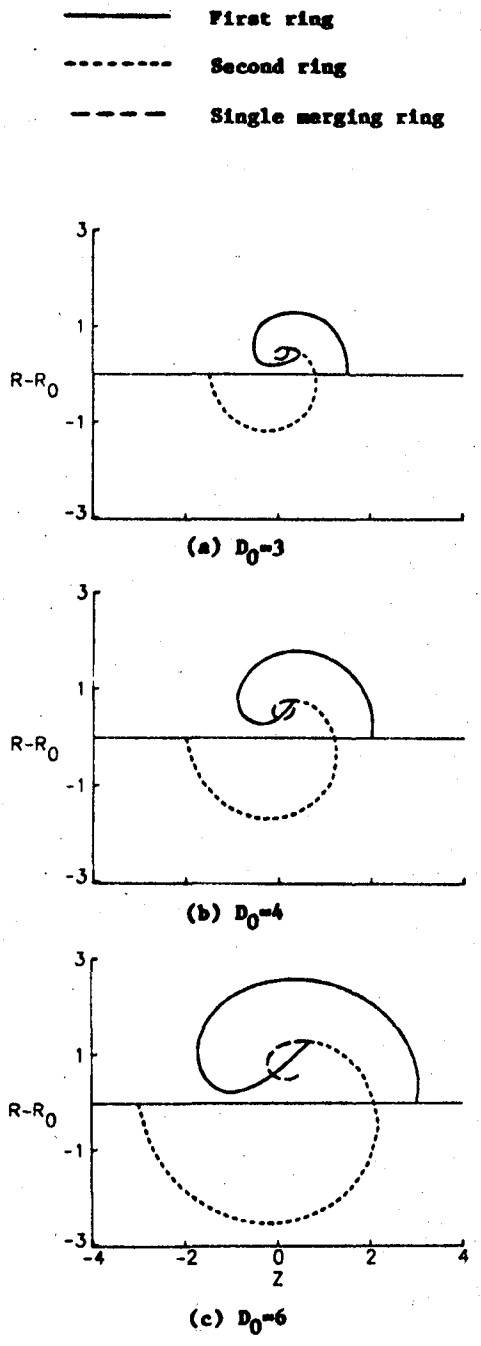

Fig. 6: Effect of initial separation distance on the trajectories of maximum vorticity for two vortex rings with R_0=15 at Re=251.

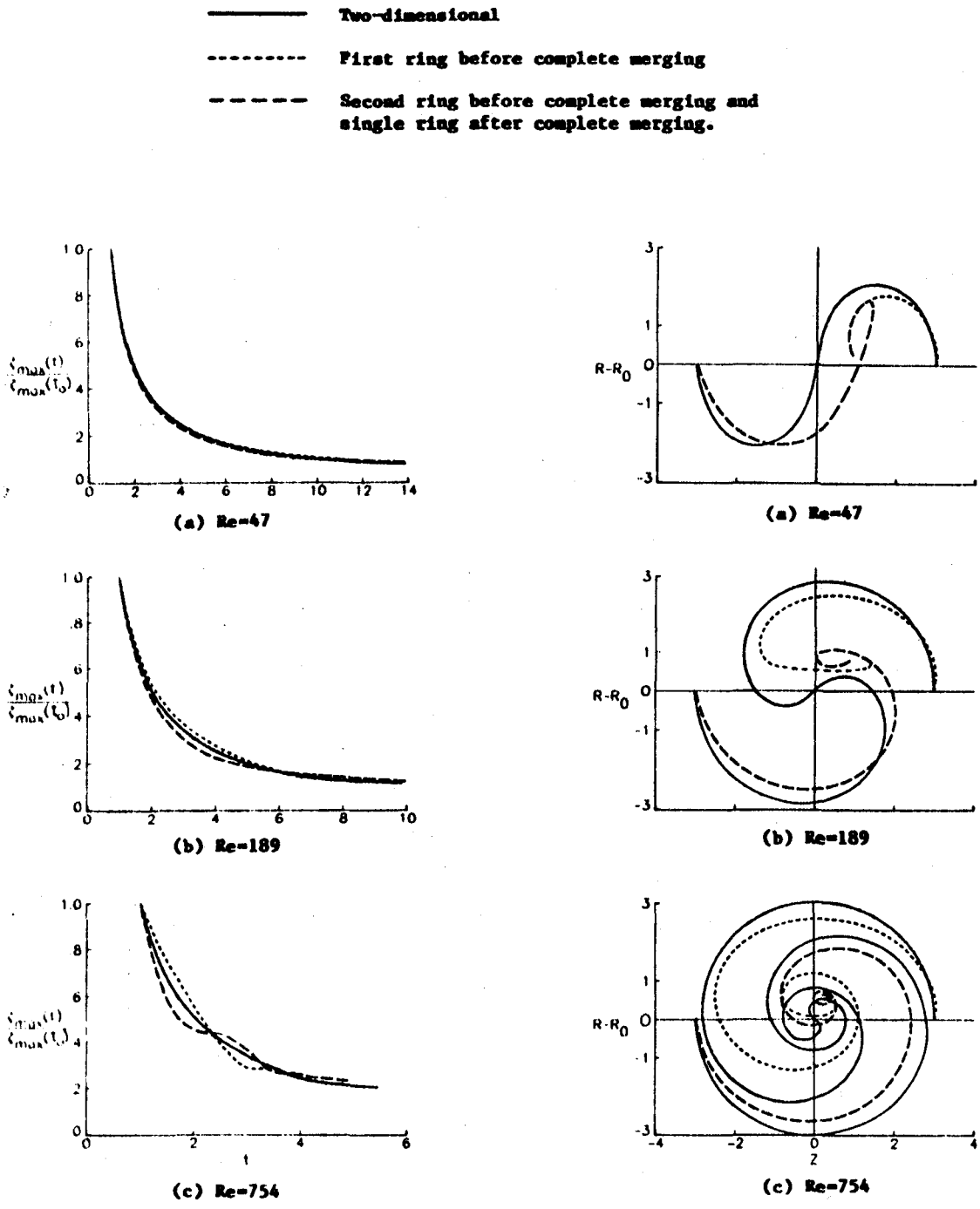

Fig. 7: Effect of Reynolds number on the decay of maximum vorticity for two vortex rings with R_0=15 and D_0=6.

Fig. 8: Effects of Reynolds number on the trajectories of maximum vorticity for two vortex rings with R_0=15 and D_0=6.

1. Report No.	2. Government Accession No.	3. Recipient's Catalog No.
NASA TM 86325		

4. Title and Subtitle	5. Report Date
NUMERICAL STUDIES OF INTERACTING VORTICES	January 1985
	6. Performing Organization Code 505-43-43-01

7. Author(s)	8. Performing Organization Report No.
Grace C. Liu and Chung-Hao Hsu *	
	10. Work Unit No.

9. Performing Organization Name and Address	11. Contract or Grant No.
NASA Langley Research Center Hampton, Virginia 23665	
	13. Type of Report and Period Covered
12. Sponsoring Agency Name and Address	Technical Memorandum
National Aeronautics and Space Administration Washington, DC 20546	14. Sponsoring Agency Code

15. Supplementary Notes

*University of Kansas
Lawrence, Kansas

16. Abstract

To get a basic understanding of the physics of flowfields modeled by vortex filaments with finite vortical cores, systematic numerical studies of the interactions of two-dimensional vortices and pairs of coaxial axisymmetric circular vortex rings were made. Finite-difference solutions of the unsteady incompressible Navier-Stokes equations were carried out using vorticity and stream function as primary variables. Special emphasis was placed on the formulation of appropriate boundary conditions necessary for the calculations in a finite computational domain. Numerical results illustrate the interaction of vortex filaments, demonstrate when and how they merge with each other, and establish the region of validity for an asymptotic analysis.

17. Key Words (Suggested by Author(s))	18. Distribution Statement
Vortex flows Navier-Stokes solutions	Unclassified - Unlimited Subject Category 34

19. Security Classif. (of this report)	20. Security Classif. (of this page)	21. No. of Pages	22. Price
Unclassified	Unclassified	15	A02

For sale by the National Technical Information Service, Springfield, Virginia 22161